Variability of the Thermohaline Circulation in an Ocean General Circulation Model Coupled to an Atmospheric Energy Balance Model

David W. Pierce,[1] K-Y Kim,[2]

and Tim P. Barnett[1]

[1] *Climate Research Division, Scripps Institution of Oceanography, La Jolla, CA*

[2] *Climate System Research Program, Texas A&M University, College Station, TX*

Submitted to the Journal of Physical Oceanography

Revised Edition, July 1995

Abstract

We examine the variability of the ocean's thermohaline circulation in a Oceanic General Circulation Model (OGCM) coupled to a two dimensional atmospheric Energy Balance Model (EBM). The EBM calculates air temperatures by balancing heat fluxes, including that from the ocean surface; air temperature and ocean circulation evolve together without imposed temperature restrictions except specification of the solar constant. The heat coupling is scale dependent such that small-scale ocean temperature anomalies are damped quickly while large-scale ones lose heat slowly by long-wave emission to space. These boundary conditions are more realistic than restoring conditions even when weak coupling is used since they allow changes in air temperature and wholesale shifts in the planetary heat balance.

It is found that coupling the EBM to the OGCM increases the stability of the ocean's thermohaline circulation. This increased stability arises from the ability of the coupled model to develop a four times greater sea surface temperature response to a given change in thermohaline overturning than when traditional restoring boundary conditions are used. The sense of this increased response works to stabilize the thermohaline overturning. The specific value of the small-scale thermal coupling coefficient also influences the stability even though the large-scale coefficient is always small (2 W m^{-2} C^{-1}); this suggests that small-scale processes might determine the large-scale stability.

1. Introduction

There has been a growing awareness in the oceanographic modeling community that the formulation of surface boundary conditions in Oceanic General Circulation Models (OGCMs) plays an important role in determining the stability of the models' thermohaline circulation. "Restoring" boundary conditions are often used: $\partial T/\partial t = \tau^{-1}(T^* - T)$ where T is an ocean tracer (temperature or salinity), τ is a prescribed time constant, and T^* is derived from observations. Stommel (1961) first pointed out that a two-box model of the thermohaline circulation with restoring boundary conditions on both temperature and salinity can have more than one steady state, if the restoring temperature and salinity have opposite tendencies on the density and different time constants are used to restore the two. In essence a "fast" meridional overturning is dominated by the agent (temperature or salinity) which acts rapidly; a "slow" overturning is dominated by the one which acts slowly. Since by assumption the two agents would drive flow in opposite directions, the sense of the fast overturning must be opposite to that of the slow overturning.

F. Bryan (1986), using the GFDL OGCM (K. Bryan 1969), explored the effect of boundary conditions on the thermohaline circulation. He used either restoring conditions with equal time constants for salinity and temperature or restoring temperature with flux salinity ("mixed") boundary conditions. Mixed boundary conditions are equivalent to restoring boundary conditions in the limit as $S^* \to \infty, \tau \to \infty$, and S^*/τ constant (Marotzke 1994). They are therefore an extreme form of the boundary conditions which Stommel used. F. Bryan found that with equal time constants the thermohaline circulation was stable with deep water production in the North Atlantic; with mixed boundary conditions sinking in the North Atlantic abruptly ceased. He termed this the “polar halocline catastrophe” since it was caused by an accumulation of freshwater capping off the water column and preventing convection. Subsequent work (see Weaver et al. (1993) for a review) has elaborated on this finding, illustrating cases of multiple steady equilibria or oscillations in the ocean’s thermohaline circulation under mixed boundary conditions.

Zhang et al. (1993) and Power et al. (1994) found that moving from mixed boundary conditions to flux conditions for both salinity *and* temperature prevented their OGCMs from exhibiting multiple equilibria. This is in accord with Stommel’s requirement that different time constants for temperature and salinity are necessary for the multiple equilibria to exist (but only when using a linear equation of state; see Pierce et al. (1995)). They also showed that increasing the restoring time constant for temperature produces a graduated transition in model behavior between the two regimes. Determining an appropriate value of this time constant then becomes of paramount importance.

The original work of Haney (1971) on which restoring boundary conditions are based and a later analysis by Oberhuber (1988) suggest a value for the air/sea temperature coupling coefficient of 30 to 40 W $m^{-2}C^{-1}$. When applied to typical OGCMs this gives restoring time scales of 30 to 60 days. However, as both Marotzke (1994) and Rahmstorf and Willebrand (1995) have noted, Haney’s original formulation assumed constant restoring atmospheric temperature—clearly not appropriate when considering large-scale changes in the thermohaline circulation. In fact Bretherton (1982) pointed out that an accurate coupling coefficient should depend on the length scale of the sea surface temperature (SST) anomaly, since small anomalies are quickly cooled by wind while large anomalies warm the overlaying atmosphere which must then cool by long wave emission to space. The coupling coefficient for the latter process is about 2 W $m^{-2}C^{-1}$—an order of magnitude smaller than the coupling coefficients quoted above. Further discussion of this is given in Marotzke (1994) and Seager et al. (1994).

Rahmstorf and Willebrand (1995) used the idea of a scale-dependent coupling coefficient to derive a new surface temperature boundary condition for OGCMs. Using a flat-bottomed OGCM with simplified forcing fields they found that the thermohaline circulation modeled with such a condition is more stable than previously supposed. They argued that large coupling coefficients, by suppressing stabilizing temperature feedbacks, unrealistically exaggerate the instability of the thermohaline circulation. The formulation still requires specifying a "climatological" atmospheric equilibrium temperature field, but long-term SST deviations of ~ 5 C from climatology are possible due to the weak coupling coefficient (3 W $m^{-2}C^{-1}$) applied to large scale anomalies.

In the work shown here we carry this idea a step further by having an atmospheric Energy Balance Model (EBM) (North et al. 1983; Kim and North 1992) calculate the restoring air temperature field given the solar constant at the top of the atmosphere. The EBM is fully coupled to an OGCM with realistic forcing fields and bathymetry: the Hamburg Large Scale Geostrophic (LSG) model (Hasselmann 1982; Mikolajewicz and Maier-Reimer 1990; Maier-Reimer et al. 1993). The physics of the coupled model is such that small scale SST anomalies are damped rapidly by diffusion while large scale ones cool slowly via long wave loss to space; thus scale-dependent coupling is an integral part of the model. Net precipitation minus evaporation (P-E) is applied as a flux condition to the OGCM.

The LSG model develops Southern Ocean thermohaline oscillations when perturbed in a variety of ways (Mikolajewicz and Maier-Reimer 1990; Barnett et al. 1994; Pierce et al. 1995). Our purpose is to examine what effect the *feedbacks* between the LSG and EBM models have on these oscillations. In earlier work Mikolajewicz and Maier-Reimer (1994) used the LSG model to show how reducing the (non-scale-dependent) thermal coupling coefficient between the LSG and a specified restoring atmospheric temperature field increases the stability of North Atlantic Deep Water (NADW) production. The work here differs in that a scale-dependent coupling coefficient is used, restoring atmospheric temperatures are calculated prognostically by the EBM rather than specified from observations, and the focus is on the Southern Ocean thermohaline variability rather than on the NADW. The particular question we consider here is whether the LSG/EBM feedbacks stabilize the thermohaline circulation and suppress the oscillations. Pierce et al. (1995, PBM hereafter) show that the physical mechanism of the oscillations is subsurface heating at intermediate depths around Antarctica followed by catastrophic overturning of the water column; we explore whether this continues to be an important effect in the coupled model. To examine these questions we reproduce a number of test cases from PBM which caused oscillations in the uncoupled LSG model but using the fully coupled LSG/EBM.

The text is arranged as follows. Section 2 describes the models: the LSG, the EBM, and the manner of coupling the two. Section 3 outlines our experimental design and contains a guide to the different experiments shown. Section 4 shows the results from the experiments. Section 5 discusses the results and examines the feedbacks between the LSG and EBM in detail. The conclusions are given in Section 6.

2. Description of the models

a. The Large Scale Geostrophic model

The Hamburg Large Scale Geostrophic (LSG) OGCM used here is a full 3-dimensional primitive equation model with realistic bathymetry and forcing fields. It has 72 longitudinal by 72 latitudinal points on an E grid and 11 vertical levels. The model is explicitly designed to examine phenomena with length scales much larger than the Rossby radius of deformation and hence neglects the nonlinear advection of momentum (Hasselmann 1982). Maier-Reimer et al. (1993) describe the model in detail and show that it does a credible job of reproducing the observed oceanic state when driven by restoring temperature and salinity boundary conditions.

The model is hydrostatic, cast in fully implicit form, and uses a full equation of state (UNESCO 1981); a convective adjustment scheme eliminates static instabilities. A simple sea ice model is included where the heat flux through the ice is inversely proportional to the thickness. Seasonally varying wind stress taken from Hellerman and Rosenstein (1983) is imposed at the ocean surface.

Mikolajewicz and Maier-Reimer (1990) showed how this model reaches a steady state when driven with monthly averaged forcing fields but develops large thermohaline oscillations when noise is added to the freshwater flux forcing field. Barnett et al. (1994) showed the effect which the spectral characteristics and geographical application of this noise have on the oscillations. Pierce et al. (1995) showed that the oscillations exist under a wide range of forcing conditions including those without added noise; they also demonstrated that the physical mechanism of the oscillations is subsurface heating around Antarctica followed by overturning of the water column. This is similar to the "deep-decoupling" oscillations which Winton and Sarachik (1993) saw in a simplified OGCM.

b. The Energy Balance Model

The EBM is similar to that used by North et al. (1983) and Kim and North (1992) to study the ice age climate. It determines air temperatures given the solar constant, atmospheric diffusivity, and various relevant albedos. A wholesale shift in climatic regime is not prevented by specification of a climatological restoring atmospheric temperature field; in particular the "ice-albedo" feedback (Budyko 1969) is included through which the modeled climate can catastrophically shift to an ice-dominated state. Since the EBM is active over land as well as ocean points it can transport heat across land and predicts a continental "snow line". The effect of changes in the Earth's orbital parameters can also be examined with the EBM (North et al. 1983). Hyde et al. (1989) shows that temperatures predicted by the EBM compare well with the predictions of an atmospheric General Circulation Model.

In order to perform integrations over the time necessary for such climate studies the atmospheric model used here makes important simplifications; the biggest one is the lack of an active treatment of atmospheric moisture so that precipitation, evaporation, and clouds are fixed in this model. This increases the computational speed of the model by several orders of magnitude at the cost of omitting changes in the atmospheric moisture transport. The actual values of precipitation and evaporation used here are the same as in PBM except for test cases where new fields are diagnosed from a coupled LSG/EBM run relaxed to observed surface salinities (Levitus 1982).

The EBM determines air temperature by balancing local atmospheric heat storage (which is small), net incoming shortwave flux, outgoing longwave flux, horizontal heat diffusion, and the atmosphere-to-ocean heat flux:

$$c_{p_a} \frac{\partial T_a(\hat{r},t)}{\partial t} = QS(x,t)a(\hat{r},t) - (A + BT_a(\hat{r},t)) + \nabla \cdot \left[c_{p_a} D(x) \nabla T_a(\hat{r},t) \right] - F_{\mathrm{oc}} \qquad (1)$$

where

c_{p_a}	is the heat capacity per unit area of the air column (considered constant);
$\hat{r}$	is a vector from the Earth's center a point on the surface;
$T_a(\hat{r}, t)$	is the atmospheric temperature at a particular point and time;
Q	is one-fourth the solar constant, which is taken to be 1360 W/m^2;
x	is the sine of latitude;
$S(x, t)$	is the normalized solar short wave distribution function;
$a(\hat{r}, t)$	is the local coalbedo;
A, B	parameterize the loss of infrared radiation to space;
$D(x)$	is the atmospheric diffusion coefficient;
F_{oc}	is the atmosphere-to-ocean heat flux.

The values of all EBM parameters are shown in Table 1.

The diffusion coefficient $D(x)$ is parameterized by the same functional form used in North et al. (1983) and Kim and North (1992): $D(x) = D_f(D_o + D_2x^2 + D_4x^4)$. The latitude-dependent diffusion is twice as large at the equator as at the poles to simulate the increased mixing efficiency of the tropical Hadley cells as compared to midlatitude eddies (Lindzen and Farrell 1977). The magnitude of D_f used here is smaller than used in the previous studies because the OGCM can advectively transport heat across latitudes, a process which had to be accomplished exclusively by atmospheric diffusion in the earlier studies. The actual value used was determined by adjusting D_f until the EBM's atmospheric heat transport was close to observations (Carissimo et al. 1985) subject to the constraint that it be large enough to suppress gridpoint noise.

The background coalbedo is parameterized as $a_{\text{back}}(x) = a_o + a_2 x^2$ based on a fit to satellite observations (Stephens et al. 1981). It is important to allow changes in the coupled ocean/atmosphere system to affect the planetary coalbedo $a(\hat{r}, t)$. Therefore it is determined by the local conditions:

$$a(\hat{r}, t) = \begin{cases} Z(\theta) a_{\text{ice}} & \text{if sea ice present and } T_a(\hat{r}, t) < T_{\text{melt}} \\ Z(\theta) a_{\text{ice\_melt}} & \text{if sea ice present and } T_a(\hat{r}, t) > T_{\text{melt}} \\ Z(\theta) a_{\text{snow}} & \text{if land and } T_a(\hat{r}, t) < T_{\text{snow}} \\ a_{\text{back}}(x) & \text{otherwise} \end{cases}$$

The values of the various coalbedos are given in Table 1. The weighting function $Z(\theta)$ takes into account the increasing reflectivity of surfaces as the zenith angle θ increases. This is already included implicitly in a_{back} by the fit to data and so is not needed in that case. As in Kleeman and Power (1994) we use the simple formula given by Paltridge and Platt (1976): $Z(\theta) = 1 - \exp(-k(90^\circ - \theta))$ with $k = 0.1$ deg^{-1}.

The atmosphere to ocean heat flux is given by $F_{\text{oc}} = \kappa(T_a - T_o)$ where T_o is the temperature of the ocean model's top gridbox. The coupling coefficient κ is 40 W m^{-2}C^{-1}. This is a traditional "large" value for the coefficient consistent with the numbers quoted in Haney (1971) and Oberhuber (1988). However since the coupling is to an atmospheric temperature which *is itself affected by the ocean's temperature* the overall result is a scale-dependent damping of SST anomalies of the kind described in Bretherton (1982). In a sensitivity study shown below we show that using κ = 20 W m^{-2}C^{-1}increases the thermohaline stability of the model despite the fact that the large-scale coupling coefficient B is always small (2 W m^{-2}C^{-1}).

The scale dependence of the thermal coupling coefficient can be seen as follows. To isolate the effect of coupling to the atmosphere neglect for the moment the effect of internal ocean processes on surface ocean temperature T_o; then $c_{p_o} \partial T_o / \partial t = F_{\mathrm{oc}}$ where c_{p_o} is the oceanic heat capacity per unit area. Let the oceanic and atmospheric temperatures be be represented as the sum of a time-average and perturbation parts: $T_o = \overline{T_o} + T_o'$ and $T_a = \overline{T_a} + T_a'$, where T_a' is the atmospheric temperature anomaly associated with the specified oceanic temperature anomaly T_o'. Making use of Eq. (1) and subtracting off the mean background state we are left with

$$c_{p_o} \frac{\partial T_o'}{\partial t} = \nabla \cdot \left[c_{p_a} D(x) \nabla T_a' \right] - B T_a' - c_{p_a} \frac{\partial T_a'}{\partial t} + (\text{solar forcing}) \tag{2}$$

The "solar forcing" term represents changes forced by the temperature perturbation; for example a temperature drop in the subpolar regions could lead to more sea ice growth, increasing the local albedo and thereby decreasing the net solar forcing. The general relation between T_o and T_a is quite complicated but in the "strongly coupled" limit $\kappa \to \infty$ then $T_o \to T_a$ and all the terms in Eq. 2 can be directly compared (note that this is the limit which Rahmstorf and Willebrand (1995) use, their Eq. 7). In this limit the third term on the right hand side, representing local heat storage in the atmosphere, cannot directly dissipate the SST anomaly since $c_{p_a} \ll c_{p_o}$. Instead the dissipation must be accomplished by the first two terms on the right hand side of Eq. 2; which is more important depends on the ratio of the two, which yields an "anomaly length scale"

$$L_a = \left(\frac{c_{p_a} D}{B}\right)^{1/2}. \tag{3}$$

Letting L be the characteristic length scale of the SST anomaly, if $L \ll L_a$ then the SST anomaly is cooled by rapid atmospheric diffusion of heat to surrounding regions. If $L \gg L_a$ then the anomaly is too large to easily diffuse away to surrounding areas and extra atmospheric heat generated by the anomaly must be lost to space by long wave radiation. These two regimes were described by Bretherton (1982) and discussed in section 3 of (Marotzke 1994).

The anomaly length scale is a function of the atmospheric parameters only; in particular it does not depend on the atmosphere/ocean thermal coupling coefficients. For the values used here (see Table 1) $L_a \sim 2600$ km at midlatitudes. This is not a free parameter; the atmospheric diffusion coefficient (D_f) was adjusted so that the model's atmospheric heat transport matched observations (Carissimo et al. 1985); the coefficient for the longwave emission to space (B) is determined by a fit to satellite observations (Stephens et al. 1981).

It is important to note that since L_a is much larger than the internal Rossby radius of deformation appropriate to oceans, motions which are "large" on the oceanic scale (i.e. many Rossby radii) can still be considered small compared to L_a. Therefore even "large-scale" oceanic motions can be effectively coupled to the atmosphere by the small-scale coupling coefficient κ rather than the large-scale coefficient B. This helps explain the coupled model's sensitivity to κ even when B is small, as demonstrated in section 4e.

It also suggests that using a value of the order of B for both the large *and* small-scale thermal coupling coefficients would be inappropriate.

Equation 2 differs from the parameterization used by Rahmstorf and Willebrand (1995) (their Eq. 11) by the inclusion of an extra forcing term which arises from changes in the incident solar insolation. This term is important in the positive ice-albedo feedback: cold polar temperatures can lead to increased sea ice, which lowers the albedo, leading to temperatures which are colder still. This effect is important on relatively short time scales over which the areal extent of sea ice changes. The solar term is also important when the time scales are extended to the point where changes in the Earth's orbital parameters begin to significantly influence the insolation, 20 to 100 kyears. Both these effects are included in the coupled LSG/EBM although we will not present results on such long time scales here. On the other hand changes in cloud cover are surely important on such time scales and would affect the heat budget via the solar insolation term; but the lack of an atmospheric moisture model precludes including such changes in this study.

c. Coupling and boundary conditions

The LSG uses a 30-day time step; the EBM uses a 1-day time step so that daily variations in solar insolation are resolved. Therefore in the coupled model the EBM is subcycled 30 times for each time step of the LSG model.

The two models interact at the LSG's surface gridbox. Surface temperature, salinity, and ice thickness are calculated using the EBM's 1-day time step; the dynamical variables are calculated using the LSG's 30-day time step. The assumption here is that surface buoyancy fluxes can effect rapid changes in surface density but that these changes affect the ocean circulation through slower processes such as the propagation of Rossby waves.

The LSG/EBM is fully coupled model with the external forcings consisting of an imposed freshwater flux field and a specified heat flux (the solar constant). A realistic long-time steady state can be achieved even when using flux coupling because for the salinity the net integrated oceanic freshwater flux is zero; for the temperature strong, physically-realistic radiative feedbacks included in the EBM prevent the temperatures from drifting too far from reality. Feedbacks on the heat flux drive the model temperatures towards a configuration which is *internally self-consistent* rather than *externally imposed*; this is similar to the "zero heat capacity" atmosphere used by Schopf (1983) to model El Niño. No internally self-consistent temperature fields (such as an ice-covered Earth) are prevented by external specification of a temperature field.

3. Experimental design

Our selection of experiments is dictated by our objectives:

1. To *isolate* the effect which coupling the LSG model to the EBM has on the LSG's thermohaline variability.

2. To determine *how robust* our conclusions are to reasonable variations in the experimental configuration.

a. Control case (CONTROL)

The "control case" has all aspects of the LSG model exactly the same as those used in PBM with the sole exception of the restoring atmospheric temperature field, which is calculated by the EBM rather than specified. This configuration addresses our primary motivation: isolating the effect of coupling the LSG to the EBM. As we show below, air temperatures evolved by the EBM are unrealistic near the Bering Strait; to ensure that our conclusions are not a spurious result of these differences, air temperatures in the region are corrected to observed values.

b. Freshwater flux noise cases (FWNOISE)

Mikolajewicz and Maier-Reimer (1990) show that adding noise to the freshwater flux field produces thermohaline variability in the LSG-only model. Since our primary objective is to asses the effect of the coupling on such variability we force the coupled LSG/EBM with a freshwater flux field with added noise. These are the "freshwater flux noise" cases.

c. Smoothed precipitation cases (SMOOTH)

PBM show that smoothing the precipitation field around Antarctica is an effective way of generating oscillations in the LSG-only model. Here we repeat those experiments using the coupled LSG/EBM. There are two different smoothed P-E cases used, denoted by “A” and “B”. Field “A” is identical to that used in PBM; the P-E field is smoothed in three regions: the Weddell Sea (70° W to 10° W), the Ross Sea (170° E to 155° W), and the Enderby Sea (10° W to 120° E), with all regions extending from the Antarctic coast to 60°S. In each of these regions instantaneous net P-E is set to the spatially averaged value over the region. Field “B” simply extends the edge of the Enderby region from 120° E to 170° E.

d. Uncorrected cases (UNCORR)

To determine the effect of the temperature correction on the results we also examine a set of experiments without any corrections whatsoever; these are the “uncorrected” cases. We show that the influence which coupling to the EBM has on the LSG’s thermohaline circulation is insensitive to whether or not the correction is applied.

e. Low-κ Case (LO-K)

We also examine the effect of the actual *value* of the small-scale thermal coupling coefficient on the results. As described previously the thermal coupling coefficient is scale dependent; the value of the large-scale coefficient is derived from satellite observations but the appropriate value of the small-scale coefficient is open to question. The original work of Haney (1971) and an analysis by Oberhuber (1988) indicate a value of 30 to 40 W m^{-2} K^{-1} but Seager et al. (1994) suggest a value closer to 15 W m^{-2} K^{-1}. We typically use a value of 40 W m^{-2} K^{-1} for the small scale thermal coupling coefficient but in the “low-κ” experiments we use 20 W m^{-2} K^{-1}.

f. New freshwater flux case (NEWFWF)

Although the control case most directly approaches our primary objective—*isolating* the effect of the EBM coupling on the LSG—there is another consideration which must be kept in mind: the freshwater flux field derived for the LSG model alone may not the best one to use with the *coupled* LSG/EBM. This is important because a mismatch between the circulation and forcing fields can contribute to thermohaline variability in OGCMs (Cai 1995). Since the temperature field evolved by the EBM is somewhat different from the field used to drive the LSG alone it may not be correctly matched to the freshwater flux field. To avoid this potential problem we examine the results of experiments ("new freshwater flux") with a freshwater flux field diagnosed from a spin up run of the coupled LSG/EBM where salinities were relaxed to observations.

4. Model results

As in PBM demonstrations of the model variability will typically be shown using a convenient proxy, the volume transport through the Drake Passage. This quantity is well correlated to the total amount of convective activity around the Antarctic continent and the maximum value of the Southern Ocean meridional overturning streamfunction. Since the wind forcing has no interannual variability, changes in Drake Passage transport do not arise from changes in the wind-driven circulation.

a. Control case (CONTROL)

In the control case of the coupled LSG/EBM no aspects of the LSG model are changed from PBM with the exception that the restoring atmospheric temperature field is predicted by the EBM rather than specified from observations.

Figure 1 shows the annually averaged temperature evolved by the EBM and the COADS data set (Woodruff et al. 1987) for comparison. The temperatures predicted by the EBM are generally in reasonable agreement with the COADS observations. The main exception to this is that the EBM's temperatures are too zonally uniform; this is especially noticeable along the east coast of South America and in the North Atlantic.

A local problem is that temperatures in the Bering Strait and Chukchi Sea are too cold. As a result sea ice forms too far south; the associated brine rejection and consequent mixing destroy the surface halocline resulting in North Pacific Intermediate Water (NPIW) which penetrates too deeply. This can be seen in a salinity section along the date line (Fig. 2). There is a tongue of fresh (34.5 psu) water which has a maximum at about 750 m but whose influence can be seen to the bottom. In the GEOSECS data this tongue is confined to the upper 1000 meters and is 0.3 psu fresher than in the model. To overcome this problem air temperatures were weighted towards observations in the region: $T_a = \gamma T_{\text{OBS.}} + (1 - \gamma)T_{\text{EBM}}$ with γ as shown in Fig. 3. Figure 4 shows the salinity section with the correction applied. The NPIW is confined to the upper 2000 meters and the strong surface halocline in the North Pacific is present. This correction is used in all cases except the "uncorrected" ones (shown below) which we use to assess the effect of this procedure on the model's behavior. It will turn out that the correction does not affect our conclusions regarding the influence of the LSG/EBM feedbacks on the stability of the model.

The sea surface temperature and salinity for the control case are shown in Fig. 5. Temperatures are in reasonable accord with observations although the overly-zonal structure is again evident. The Pacific warm pool is within 0.75 C of observations while temperatures around Antarctica are somewhat too warm. In general the EBM has difficulty representing the extremely low temperatures on the Antarctic continent; this is not a problem here as we are most concerned with oceanic temperatures and temperatures on the Antarctic continent are cold enough to guarantee the presence of snow (with its consequent high albedo). However the diffusive nature of the EBM tends to make the immediately adjoining ocean regions too warm; as a result sea ice around Antarctica is too thin, averaging about 0.2 m versus 0.5 to 0.6 m from observations (Wadhams et al. 1987).

The barotropic stream function for the control case is shown in Fig. 6. As expected the western boundary currents are underrepresented due to the coarse resolution of the LSG model. However they are not significantly different from the results obtained with restoring boundary conditions as shown in Maier-Reimer et al. (1993). The meridional circulations for the global, Atlantic, and Pacific oceans are shown in Fig. 7. The Southern Ocean deep water sources are somewhat weak, producing about 5 to 10 Sv (Sv = 10^6 m^3 s^{-1}) of deep water; about 20 Sv of water sinks in the North Atlantic near 62° N.

Figure 8 shows the atmosphere's meridional heat transport in the EBM and from observations. The model is slightly too diffusive resulting in a heat transport which is about 17% too large. (Reducing the EBM's diffusion constant much further caused the EBM to diverge). This implies that the anomaly length scale estimate of $L_a \sim 2600$ km from Eq. 3 is somewhat too large; but note that L_a is only weakly dependent on the diffusion constant.

Figure 9 shows the Drake Passage transport for the control case. After the initial transient there is no evidence of thermohaline variability. Thus the coupled model develops a steady state global ocean/atmosphere climate.

b. Noise in freshwater flux (FWNOISE)

Mikolajewicz and Maier-Reimer (1990) showed that adding noise to the freshwater flux driving the LSG model stimulates strong thermohaline oscillations with a period of about 300 years and an amplitude (in Drake Passage transport) of about 90 Sv. Barnett et al. (1994) showed that there is a threshold for this effect to occur; white noise with a standard deviation of 0.5 mm day^{-1} did not stimulate the oscillations but with a standard deviation of 1.0 mm day^{-1} or greater did.

Adding white noise to the freshwater flux field with standard deviations up to an unrealistically large 10 mm day^{-1} does *not* generate thermohaline fluctuations in the coupled LSG/EBM. The Drake Passage transport for the case with 10 mm day^{-1} is shown in Fig. 10 (solid line) along with the Drake Passage transport for the LSG model alone driven by 2 mm day^{-1} of noise (dashed line) for comparison. Thus *coupling the LSG model to the EBM substantially increases the stability of the LSG's thermohaline circulation*. As further discussed in section 5 this is due to the role of negative temperature feedbacks in stabilizing the thermohaline overturning (Rahmstorf and Willebrand 1995): more overturning means more warm water is advected into the convection region, slowing the overturning. Less overturning means less warm water is advected into the area, speeding the overturning. This feedback is active in the coupled LSG/EBM and therefore the thermohaline circulation is more stable; when the LSG is relaxed to a specified temperature field with $\kappa \sim 40$ W m^{-2} K^{-1} temperatures can vary by only a small amount and so temperature-driven changes in density are too small to have much effect.

c. Smoothed precipitation fields (SMOOTH)

PBM showed that using smoothed P-E field “A” (as described in section 3c) stimulated oscillations in the LSG-only model. The same forcing field did *not* stimulate any oscillations in the coupled LSG/EBM. Again this shows that coupling to the EBM has increased the stability of the LSG's thermohaline circulation.

It is still possible to generate oscillations in the coupled LSG/EBM, however. For example Fig. 11 shows the Drake Passage transport using smoothed P-E field “B” (described in section 3c) which has more smoothing around Antarctica than field “A” (it should be noted that the actual P-E field around Antarctica is poorly known). Thermohaline oscillations with a peak to peak amplitude of about 70 Sv are generated in this case. An analysis of the oscillations show that they are characterized by the same physical mechanism as found in PBM: subsurface heating around the Antarctic continent eventually destabilizing the water column and triggering convective overturning. The heat is vented to the atmosphere, then the net positive P-E freshens the surface waters, stratifying the water column; convection slows and the cycle repeats. Thus *the physical mechanism of thermohaline variability is still present*; it must be the coupling to the EBM which prevents the oscillations from occurring as readily.

d. Uncorrected case (UNCORR)

In the preceding section temperatures in the region of the Bering Strait and Chukchi Sea were set to observed values. To understand what effect this has on the stability of the thermohaline circulation we examined several test cases which did not have this correction.

Figure 12 (solid line) shows the Drake Passage transport for an experiment identical to the control case except without any temperature correction. This configuration is not as stable as when the corrections are used; there are periodic drops in the transport which occur when freshwater accumulates in the surface waters around Antarctica, shutting off convection. The period between such cessations is about twice as long as in the noise-forced cases of Mikolajewicz and Maier-Reimer (1994) and Barnett et al. (1994) and the smoothed precipitation cases of PBM.

Applying white noise with a standard deviation of 5 mm day^{-1} to the freshwater flux driving the uncorrected LSG/EBM (Fig. 12, dashed line) generates less variability than when such noise is applied to the LSG model alone (Fig. 10, dashed line). Thus while the temperature correction is stabilizing the thermohaline circulation to some degree coupling to the EBM has a distinct stabilizing effect in and of itself. This is also seen in the “new freshwater flux” cases shown below.

e. Low-κ case (LO-K)

In the previous experiments the small-scale thermal coupling coefficient κ was 40 W m^{-2} K^{-1}. To examine the sensitivity of the results to this value we tried test cases with κ = 20 W m^{-2} K^{-1}. The large-scale coefficient was kept at 2 W m^{-2} K^{-1} throughout. As our interest is primarily in what effect this change has on the LSG/EBM's thermohaline oscillations we only examine two cases, both of which oscillated; the case with P-E smoothed field "B" (Fig. 11); and the uncorrected case with P-E smoothed field "A". Figure 13 shows the Drake Passage transport for these two cases with low values of κ: reducing the value of κ eliminates the oscillations. Therefore we see that *even though the large-scale thermal coupling coefficient is always small the small-scale coefficient can determine the stability of the system.* This suggests that processes with characteristic lengths less than the anomaly length scale L_a (about 2600 km here) are crucial in generating the large-scale variability. An obvious candidate for this process is oceanic convection, which occurs on a considerably smaller characteristic scale (Jones and Marshall 1993).

f. New freshwater flux case (NEWFWF)

The previous results were obtained using the same freshwater flux field as in PBM. This was done so that the effect of coupling the LSG model to the EBM could be examined in isolation. However it is reasonable to require that the forcing freshwater flux field be rederived for the coupled LSG/EBM so that the atmospheric freshwater flux and heat flux can be simultaneously consistent with the evolved ocean circulation. To this end we tried a number of test cases with a new freshwater flux field diagnosed from a spin up run of the coupled LSG/EBM with surface salinities relaxed to observed values (Levitus 1982).

Figure 14 shows the Drake Passage transport for the new freshwater flux case both with and without the temperature correction. Comparing Figs. 14 and 12 it can be seen that the uncorrected case with the new freshwater flux has less variability than the uncorrected case with the original freshwater flux.

The result of adding white noise with a unrealistically large standard deviation of 5 mm day^{-1} to both the corrected and uncorrected cases with the new freshwater flux field is shown in Fig. 15. The noise does not cause the coupled LSG/EBM to oscillate despite the fact that one fifth this amount of noise caused the LSG-only model to oscillate. Again we see that coupling the LSG model to the EBM has stabilized the thermohaline circulation in both the corrected and uncorrected cases.

5. Discussion

The discussion in PBM points out how it is possible for the LSG model to oscillate due to the closeness of two buoyancy fluxes: the destabilizing heating across the Antarctic Circumpolar Current (ACC) and the stabilizing positive P-E south of the ACC. If the magnitudes of the two buoyancy fluxes are not sufficiently similar then the larger one will dominate; only if they are reasonably close will the oscillations be self-sustaining.

The results shown here indicate that such closeness of buoyancy fluxes, although necessary, is not sufficient to produce oscillations. The coupled LSG/EBM can indeed be induced to oscillate (as shown in Fig. 11); however forcings which generated oscillations in the LSG-only model, such as noise added to the freshwater flux, did not do so in the coupled LSG/EBM. And yet the heat flux across the ACC in the coupled LSG/EBM is about the same as in the uncoupled model (1.46 vs. 1.50 PW); and the buoyancy fluxes due to net freshwater input are exactly the same (except in the "new freshwater flux" cases). Thus the buoyancy fluxes in the LSG/EBM are close to those which produced oscillations in the LSG-only model yet such oscillations are much harder to produce in the LSG/EBM.

The feedbacks associated with the LSG's coupling to the EBM must be responsible for this added stability. Rahmstorf and Willebrand (1995) describe how a negative temperature feedback present when the thermal coupling coefficient is small can stabilize the thermohaline overturning: a weakened thermohaline overturning reduces the poleward heat transport, leading to colder high-latitude surface temperatures, and therefore greater surface densities, more convection and increased thermohaline overturning. Conversely a strengthened meridional overturning increases the poleward heat transport, warming the surface waters, thereby decreasing the surface density and reducing the strength of the overturning. Thus this feedback is in the proper sense to explain the observation from section 4 that the coupled LSG/EBM's thermohaline circulation is more stable than in the uncoupled model.

The hypothesis that the negative temperature feedback described above is the cause of the greater thermohaline stability in the coupled LSG/EBM can be tested using the results from section 4. To test this we will address two questions: 1) Is the feedback *present* in the coupled LSG/EBM? If so, then the feedback might account for the greater stability; if not present then it cannot account for the stability. 2) If the feedback is present, then is it *strong enough* to account for the substantially greater stability of the LSG/EBM compared to the LSG-only model?

To address the first question we note that a given change in thermohaline overturning will generate a larger change in high latitude surface temperature when the feedback is present than when it is absent. Therefore to test whether the feedback is present we will examine the correlation of (changes in thermohaline overturning) to (changes in high latitude surface temperature) for the coupled LSG/EBM and the LSG-only model. As shown below it turns out that the negative temperature feedback is present in the coupled LSG/EBM.

To address the second question we examine the effect which the feedback has on high-latitude surface *densities*. Changes in surface temperature due to the negative feedback directly change the surface density as described by the equation of state. Only if the changes in surface density due to the feedback are a substantial fraction of the background density stratification will the feedback have a strong influence on the high latitude water column stability, and thus on the thermohaline overturning rate. As shown below it turns out that the feedback is strong enough to account for the difference in thermohaline stability between the LSG/EBM and the LSG-only models.

First we will determine if the negative temperature feedback is present in the coupled LSG/EBM. If so then a given change in thermohaline overturning will generate a larger change in high latitude surface temperature in the coupled LSG/EBM than in the LSG-only model. Figure 16 shows the relation between changes in Drake Passage transport (acting as a proxy for the rate of Southern Ocean thermohaline overturning) and changes in average Southern Ocean temperature south of 60° S. The changes were obtained by center differencing the respective time series over a span of 10 years. Two cases are shown:

one from the coupled LSG/EBM (Fig. 11) and one using the LSG-only model forced with 2 mm day^{-1} of white noise added to the freshwater flux field. The results show that a given change in overturning produces about four times as much change in surface temperature in the coupled LSG/EBM as in the LSG only. We therefore conclude that the negative temperature feedback is present in the coupled LSG/EBM.

It remains to be determined how strong an effect the negative temperature feedback is. As shown above the feedback results in larger excursions of surface temperature in the high latitudes; this implies larger excursions of surface density. If the changes in surface density produced by the feedback are small compared to the background density stratification then the feedback will have little effect on the stability of the water column and thus the thermohaline overturning rate. If the changes in surface density are large then the feedback will have a significant effect on the overturning rate. The typical change in surface potential density $\Delta\sigma_o$ due to the feedback can be estimated as $\alpha\Delta T$ where ΔT is the typical change in surface temperature due to the negative temperature feedback and α is the thermal expansion coefficient. Typical temperature variations seen with and without the temperature feedback can be estimated from Fig. 16; this gives $\Delta T \sim$ 0.74 C for the LSG/EBM case and $\Delta T \sim$ 0.13 C for the LSG-only model. For seawater at 1 C and 34 psu α = 0.0658 kg m^{-3} K^{-1}. Therefore $\Delta\sigma_o$ = 0.0487 kg m^{-3} for the coupled LSG/EBM but only 0.0086 kg m^{-3} for the LSG model alone. Figure 17 shows the potential density (referenced to the surface) for the top 500 m of the water column from the control case of the coupled LSG/EBM. The location plotted is in the middle of the Enderby sector around Antarctica; this spot was chosen because PBM show that the oscillations in the LSG-only model start in the Enderby. Also shown are $\Delta\sigma_o$ for the LSG/EBM model and

LSG-only model. It is clear that the change in $\Delta\sigma_o$ seen when coupling to the EBM is in the proper range to be an important effect; i.e. in the LSG-only case $\Delta\sigma_o$ appears too small (compared to the background stratification) to be an important influence on density, but it is significant when the EBM feedbacks are included. Recall that the estimates of temperature variability were taken from averaged temperature fields which underrepresent the degree of variability; the true values of $\Delta\sigma_o$ are somewhat larger than shown.

The results show that the negative temperature feedback is: 1) in the proper sense to explain the increased themohaline stability of the coupled LSG/EBM compared to the LSG-only model; 2) actually present in the coupled LSG/EBM; 3) strong enough to affect the thermohaline stability of the coupled LSG/EBM. We therefore conclude that it is the negative temperature feedback which accounts for the increased thermohaline stability of the coupled LSG/EBM model. Furthermore these results provide strong support for the idea that restoring boundary conditions on temperature with large restoration coefficients unrealistically exaggerate the instability of the thermohaline circulation through neglect of this feedback.

6. Conclusions

We have examined the results of coupling an atmospheric Energy Balance Model (EBM) to the Hamburg Large Scale Geostrophic (LSG) OGCM. This coupling means that the air temperatures driving the LSG model are calculated prognostically rather than being specified from observations. Moreover the coupling is applied in such a way that small-scale sea surface temperature anomalies cool rapidly while large-scale ones cool slowly.

The EBM generally produces air temperatures which are in reasonable accord with observations although too zonally uniform. The Bering Strait and Chukchi Sea are the exception to this; temperatures there are too cold. The main result of this deficiency is the elimination of the surface halocline in the North Pacific and the consequent increase in depth of penetration of North Pacific Intermediate Water. This regional shortcoming does not affect the main conclusions of this work, which are:

1. *The thermohaline circulation of the LSG model is more stable when coupled to the EBM.* Forcings which were sufficient to stimulate thermohaline variability in the LSG model with mixed boundary conditions—such as white noise added to the freshwater flux field—do not do so in the coupled LSG/EBM. This was true whether or not temperatures were corrected in the Bering Strait and whether the original or a rederived freshwater flux forcing field was used.

2. *It is still possible to generate the thermohaline variability in the coupled LSG/EBM*. Smoothing the P-E field over a wide region around Antarctica still produces oscillations in the coupled model; the evolution of the oscillations is the same as for the LSG model using mixed boundary conditions (Pierce et al. 1995). Therefore we conclude that the coupling does not eliminate the physical mechanism responsible for the oscillations but rather adds feedbacks which tend to suppress them.

3. *Negative temperature feedbacks are important for stabilizing the thermohaline overturning in the LSG/EBM*. The feedback is as described in Rahmstorf and Willebrand (1995): an increase in thermohaline overturning means more warm water is advected into the convection region, lowering

the density of the surface waters, and therefore slowing the overturning; a decrease in overturning means less warm water is advected into the area, cooling the surface waters, increasing the surface density, and speeding the overturning. The feedback thus stabilizes the rate of overturning. The same change in overturning produces four times more sea surface temperature change in the LSG/EBM than in the LSG model alone. The density changes associated with these larger temperatures changes in the LSG/EBM are big enough to significantly influence the overall stratification whereas they are not large enough to do so when mixed boundary conditions with a large coupling coefficient are used.

4. *Reducing the value of the small scale thermal coupling coefficient from 40 to 20 W* m^{-2} K^{-1} *eliminates the thermohaline oscillations altogether.* This is true whether or not temperature corrections were applied and despite the fact that the large-scale coupling coefficient was always small (2 W m^{-2} K^{-1}). This means that the value of the small-scale coefficient must be determined carefully even when a scale-dependent thermal coupling is used. Mikolajewicz and Maier-Reimer (1994) have shown that in the LSG-only model reducing the (non-scale-dependent) thermal coupling coefficient decreases the thermohaline variability in the model. Together with these results this implies that small-scale processes can have a determining influence on the large-scale stability. This might be related to the fact that the anomaly length scale L_a (Eq. 3) is set by *atmospheric* characteristics rather than oceanic ones. Sea surface temperature anomalies smaller than L_a cool rapidly by wind

while those larger than L_a heat the atmosphere which then cools slowly by radiating to space. Since the Rossby radius of deformation in the atmosphere is typically much larger than in the oceans, a constraint on oceanic processes which are "small" on an atmospheric scale is not as restrictive as it might be.

Acknowledgments

We would like to thank Gerry North of Texas A&M University for valuable discussions on this topic. This research was supported by DOE CHAMMP contracts DE-FG03-91-ER61215 to Scripps and DE-FG05-91ER61736 to Texas A&M, the National Science Foundation under grant NSF ATM 93-14495, the Scripps Institution of Oceanography, and sponsored in part by the University of California and Digital Equipment Corporation under Research Grant No. 1243 (the Sequoia Project). We especially thank Uwe Mikolajewicz for making the LSG code available to us; without it this work would not have been possible.

REFERENCES

Barnett, T. P., M. Chu, R. Wilde, and U. Mikolajewicz, 1994: Low frequency ocean variability induced by stochastic forcing of various colors. In *Proceedings of the Nat. Res. Council Workshop on Decade to CenturyTimescales of Climate Variability, Irvine, CA, Sep. 21-25, 1992*. In Press.

Bretherton, F. P., 1982: Ocean Climate Modeling . *Prog. Oceanog.*, **11**, 93–129.

Bryan, F., 1986: High-latitude salinity effects and interhemispheric thermohaline circulations. *Nature*, **323**, 301–304.

Bryan, K., 1969: A numerical method for the study of the circulation of the world ocean. *J. Comp. Physics*, **4**, 347–376.

Budyko, M. I., 1969: The effect of solar radiation variations on the climate of the earth. *Tellus*, **21**, 611–619.

Cai, W., 1995: Interdecadal Variability Driven by Mismatch Between Surface Flux Forcing and Oceanic Freshwater/Heat Transport. *J. Phys. Oceanogr., in press*.

Carissimo, B. C., A. H. Oort, and T. H. Vonder Haar, 1985: Estimating the meridional energy transports in the atmosphere and oceans. *J. Phys. Oceanogr.*, **15**, 82–91.

Genthon, C., 1994: Antarctic climate modeling with general circulation models of the atmosphere. *J. Geophys. Res.*, **99**, 12953–12961.

Haney, R. L., 1971: Surface thermal boundary conditions for ocean circulation models. *J. Phys. Oceanogr.*, **1**, 241–248.

Hasselmann, K., 1982: An ocean model for climate variability studies . *Prog. Oceanogr.*, **11**, 69–92.

Hellerman, S. and M. Rosenstein, 1983: Normal monthly wind stress over the World Ocean with error estimates . *J. Phys. Oceanogr.*, **13**, 1093–1104.

Hyde, W. T., T. J. Crowley, K.-Y. Kim, and G. R. North, 1989: Comparison of CGM and Energy Balance Model Simulations of Seasonal Temperature Changes over the Past 18 000 Years. *J. Climate*, **2**, 864–887.

Jones, H. and J. Marshall, 1993: Convection with Rotation in a Neutral Ocean: A Study of Open-Ocean Deep Convection. *J. Phys. Oceanogr.*, **23**, 1009–1039.

Kim, K.-Y. and G. R. North, 1992: Seasonal Cycle and Second-Moment Statistics of a Simple Coupled Climate System. *J. Geophys. Res.*, **97**, 20437–20448.

Kleeman, R. and S. B. Power, 1994: A simple atmospheric model of surface heat flux for use in ocean modeling studies. *J. Phys. Oceanogr., in press*.

Levitus, S., 1982: Climatological atlas of the world ocean . Technical report, U.S. Dept. of Commerce, NOAA, 173 pp.

Lindzen, R. S. and B. Farrell, 1977: Some realistic modifications of simple climate models . *J. Atmos. Sci.*, **34**, 1487–1501.

Maier-Reimer, E., U. Mikolajewicz, and K. Hasselmann, 1993: Mean circulation of the Hamburg LSG OGCM and its sensitivity to the thermohaline surface forcing. *J. Phys. Oceanogr.*, **23**, 731–757.

Marotzke, J., 1994: Ocean models in climate problems . In *Ocean Processes in Climate Dynamics: Global and Mediterranean Examples*, Malanotte-Rizzoli, P. and Robinson, A. R., editors. Kluwer Academic Publishers, 79–109.

Mikolajewicz, U. and E. Maier-Reimer, 1990: Internal secular variability in an ocean general circulation model . *Climate Dyn.*, **4**, 145–156.

Mikolajewicz, U. and E. Maier-Reimer, 1994: Mixed boundary conditions in ocean general circulation models and their influence on the stability of the model's conveyor belt. *J. Geophys. Res.*, **99**, 22633–22644.

North, G. R., J. G. Mengel, and D. A. Short, 1983: Simple Energy Balance Model Resolving the Seasona and the Continents: Application to the Astronomical Theory of Ice Ages. *J. Geophys. Res.*, **88**, 6576–6586.

Oberhuber, J. M., 1988: An atlas based on the COADS dataset: The budgets of heat, buoyancy and turbulent kinetic energy at the surface of the global ocean. Technical report, Max Planck Institut fur Meteorologie, Hamburg, Germany. Technical Report 15.

Paltridge, G. W. and C. M. R. Platt, 1976: *Radiative Processes in Meteorology and Climatology* . Elsevier, 318 pp.

Pierce, D. W., T. P. Barnett, and U. Mikolajewicz, 1995: On the Competing Roles of Heat and Fresh Water Flux in Forcing Thermohaline Oscillations. *J. Phys. Oceanogr., in press*.

Power, S. B., A. M. Moore, D. A. Post, N. R. Smith, and R. Kleeman, 1994: Stability of North Atlantic Deep Water Formation in a Global Ocean General Circulation Model. *J. Phys. Oceanogr.*, **24**, 904–916.

Rahmstorf, S. and J. Willebrand, 1995: The role of temperature feedback in stabilising the thermohaline circulation. *J. Phys. Oceanog., in press*.

Schopf, P. S., 1983: On Equatorial Waves and El Niño. II: Effect of Air-Sea Thermal Coupling. *J. Phys. Oceanogr.*, **13**, 1878–1893.

Seager, R., Y. Kushnir, and M. A. Cane, 1994: A note on heat flux boundary conditions for ocean models . *J. Phys. Oceanogr., submitted*.

Stephens, G. L., G. G. Campbell, and T. H. Vonder Haar, 1981: Earth Radiation Budgets . *J. Geophys. Res.*, **86**, 9739–9760.

Stommel, H., 1961: Thermohaline convection with two stable regimes of flow . *Tellus*, **13**, 224–230.

UNESCO, 1981: Unesco technical paper in marine science number 36 . Technical report, UNESCO.

Wadhams, P., M. A. Lange, and S. F. Ackley, 1987: The ice thickness distribution across the atlantic sector of the antarctic ocean in midwinter . *J. Geophys. Res.*, **92**, 14535–14552.

Weaver, A. J., J. Marotzke, E. Sarachik, and P. Cummins, 1993: Stability and variability of the thermohaline circulation . *J. Phys. Oceanogr.*, **23**, 39–60.

Winton, M. and E. S. Sarachik, 1993: Thermohaline oscillations induced by strong steady salinity forcing of ocean general circulation models. *J. Phys. Oceanogr.*, **23**, 1389–1410.

Woodruff, S. D., R. J. Slutz, R. L. Jenne, and P. M. Steurer, 1987: A comprehensive ocean-atmosphere dataset . *Bull. Amer. Meteor. Soc.*, **68**, 1239–1250.

Zhang, S., R. J. Greatbatch, and C. A. Lin, 1993: A Reexamination of the Polar Halocline Catastrophe and Implications for Coupled Ocean-Atmosphere Modeling. *J. Phys. Oceanogr.*, **23**, 287–299.

Table Captions

Table 1. Values of parameters used in the Energy Balance Model (EBM).

Figure Captions

Fig. 1. Annually averaged surface atmospheric temperature for the COADS data set (based on ship observations) and the Energy Balance Model.

Fig. 2. Salinity section along 180 W in the coupled LSG/EBM, showing the overly salty and deep North Pacific Intermediate Water.

Fig. 3. Weighting coefficient for the correction to observed temperatures in the Bering Strait and Chukchi Sea.

Fig. 4. Salinity section along 180 W in the coupled LSG/EBM with corrected temperatures showing the improved representation of North Pacific Intermediate Water when the temperature correction is applied.

Fig. 5. Surface temperature (C) and salinity (ppt) for the control case of the coupled LSG/EBM.

Fig. 6. Barotropic stream function (Sv) for the control case of the coupled LSG/EBM.

Fig. 7. Meridional overturning stream function (Sv) for the control case of the coupled LSG/EBM. Top: all oceans. Middle: Atlantic. Bottom: Pacific.

Fig.8. Meridional atmospheric heat flux in the Energy Balance Model, and observations from Carissimo et al. (1985) for comparison.

Fig. 9. Volume transport (Sv) through the Drake Passage for the coupled LSG/EBM model, control case. There is no evidence of persistent thermohaline variability.

Fig. 10. Solid line: volume transport (Sv) through the Drake Passage in the LSG/EBM when white noise with a standard deviation of 10 mm day^{-1} is added to the freshwater flux field. Dashed line: same

for the LSG-only model with 2 mm day^{-1} of noise.

Fig. 11. Volume transport (Sv) through the Drake Passage for the coupled LSG/EBM model, with smoothed net P-E around Antarctica.

Fig. 12. Volume transport (Sv) through the Drake Passage for the coupled LSG/EBM model with no temperature corrections whatsoever. Solid line: using the standard freshwater forcing field. Dashed line: with white noise with a standard deviation of 5 mm day-1 added to the freshwater forcing field.

Fig. 13. Volume transport (Sv) through the Drake Passage for the LSG/EBM model with the small-scale thermal coupling coefficient reduced from 40 to 20 W m^{-2} K^{-1}. These cases previously developed large oscillations.

Fig. 14. Volume transport (Sv) through the Drake Passage for the LSG/EBM model with a rederived freshwater flux field. Solid line: no temperature correction. Dashed line: with temperature correction.

Fig. 15. Volume transport (Sv) through the Drake Passage for the LSG/EBM model with the rederived freshwater flux field and white noise with a standard deviation of 5 mm day^{-1} added to the freshwater flux. Solid line: with temperature correction. Dashed line: no temperature correction.

Fig. 16. Correlation between change in Drake Passage transport (acting as a proxy for thermohaline overturning), and change in average surface temperature south of 60° S. Top: For the coupled LSG/EBM model. Bottom: For the LSG model alone. A given change in overturning generates four times more change in temperature in the coupled LSG/EBM than in the LSG model alone.

Fig. 17. Potential density (referenced to the surface) as a function of depth, in the Enderby sector

around Antarctica. Also shown are $\Delta\sigma_o$, the change in density produced by typical temperature variations, for the LSG/EBM and LSG-only models.

Energy Balance Model Parameters

Symbol	Value	Reference
A	203.3 W m^{-2}	North et al. (1983)
B	2.094 W m^{-2}C^{-1}	North et al. (1983)
c_p	5×10^6 J m^{-2}C^{-1}	North et al. (1983)
D_f	$\sim 3 \times 10^6$ m^{2}s^{-1}	present study
D_o	0.81	North et al. (1983)
D_2	-1.08	present study
D_4	0.74	present study
a_o	0.75	Stephens et al. (1981)
a_2	-0.18	Stephens et al. (1981)
a_{ice}	0.38	present study
a_{ice_melt}	0.28	present study
a_{snow}	0.7 (.8 in Antarctica)	Genthon (1994)
T_{melt}	-1.0	present study
T_{snow}	-10.0	present study

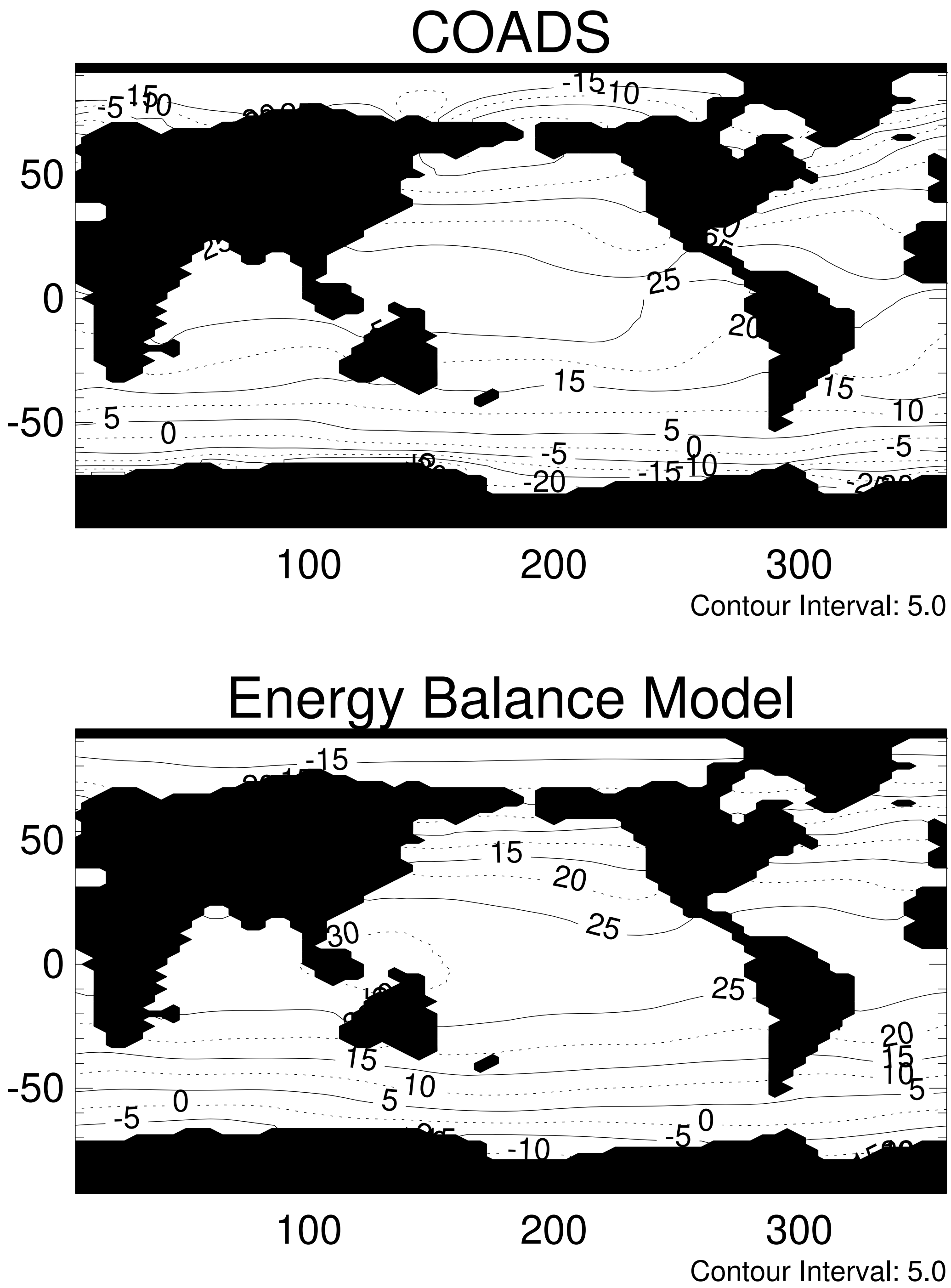
COADS
50
0
-50
100
200
300
Contour Interval: 5.0
Energy Balance Model
50
0
-50
100
200
300
Contour Interval: 5.0

Figure 1:

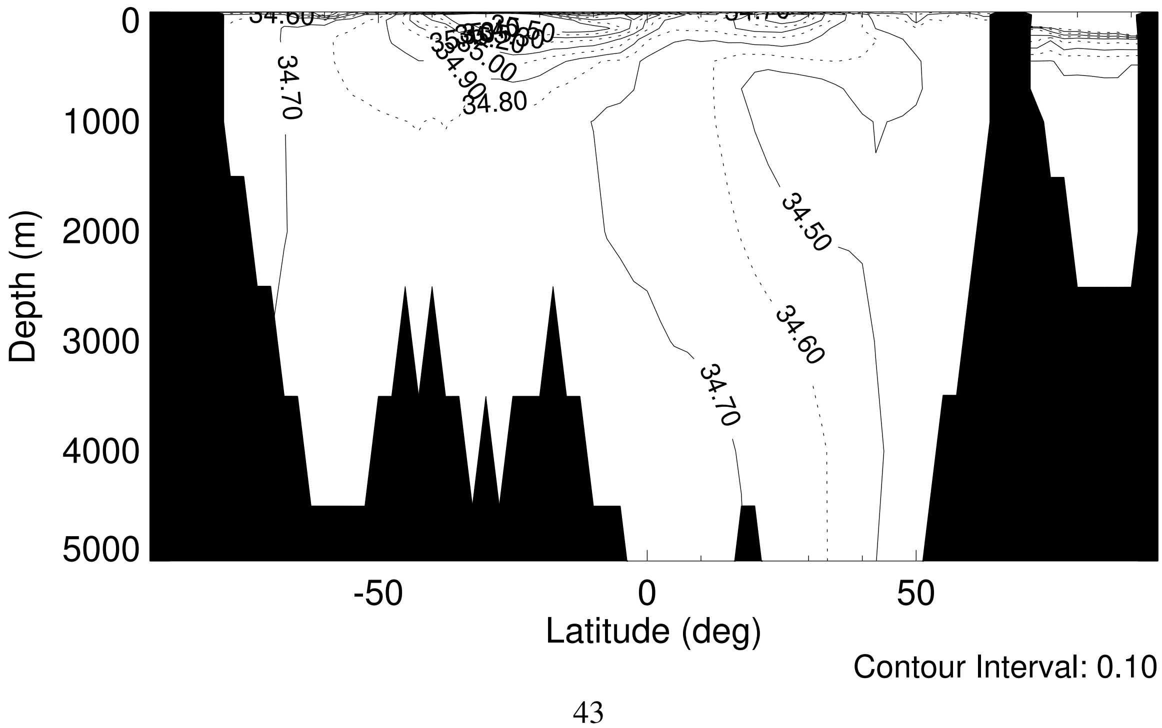

Depth (m)
0
1000
2000
3000
4000
5000
-50
0
50
Latitude (deg)
34.60
34.70
34.90
35.00
34.80
34.50
34.60
34.70
Contour Interval: 0.10

Figure 2:

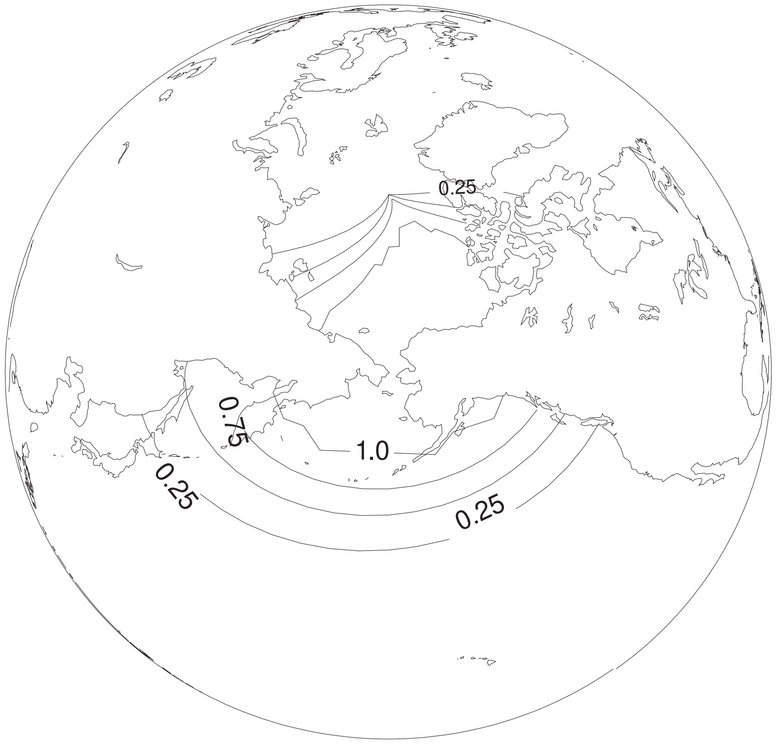

Figure 3:

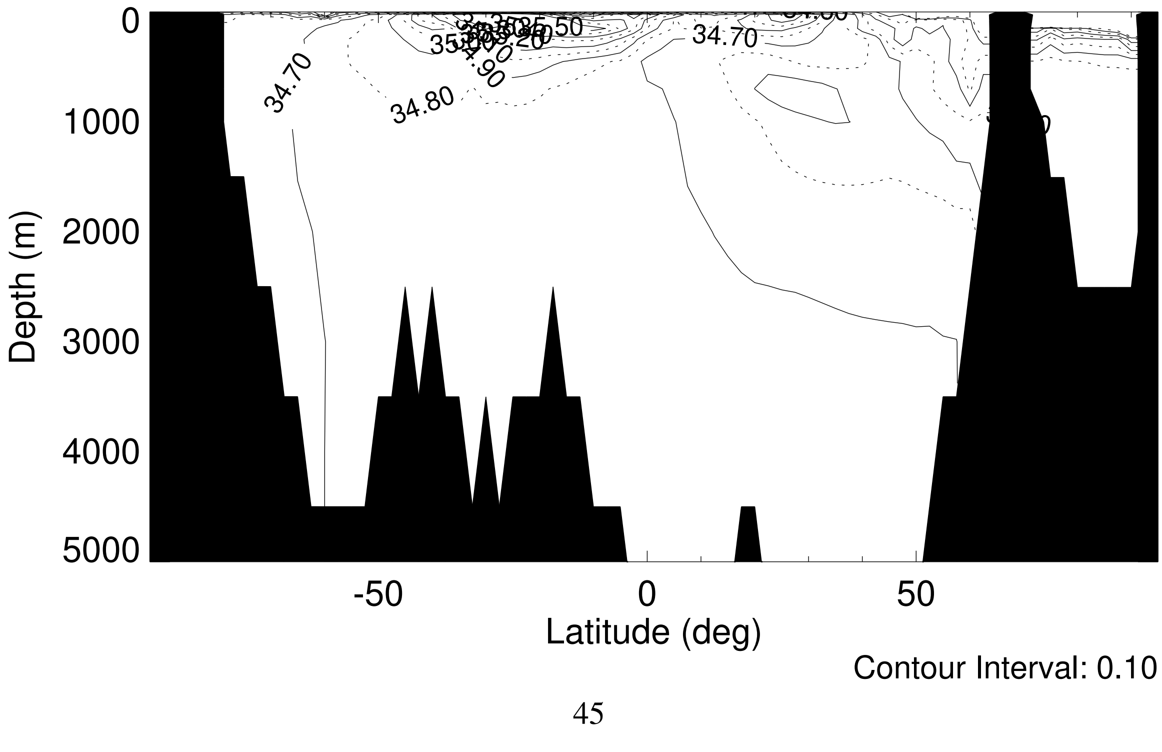
0
1000
2000
3000
4000
5000
Depth (m)
-50
0
50
Latitude (deg)
34.70
34.80
34.70
Contour Interval: 0.10

Figure 4:

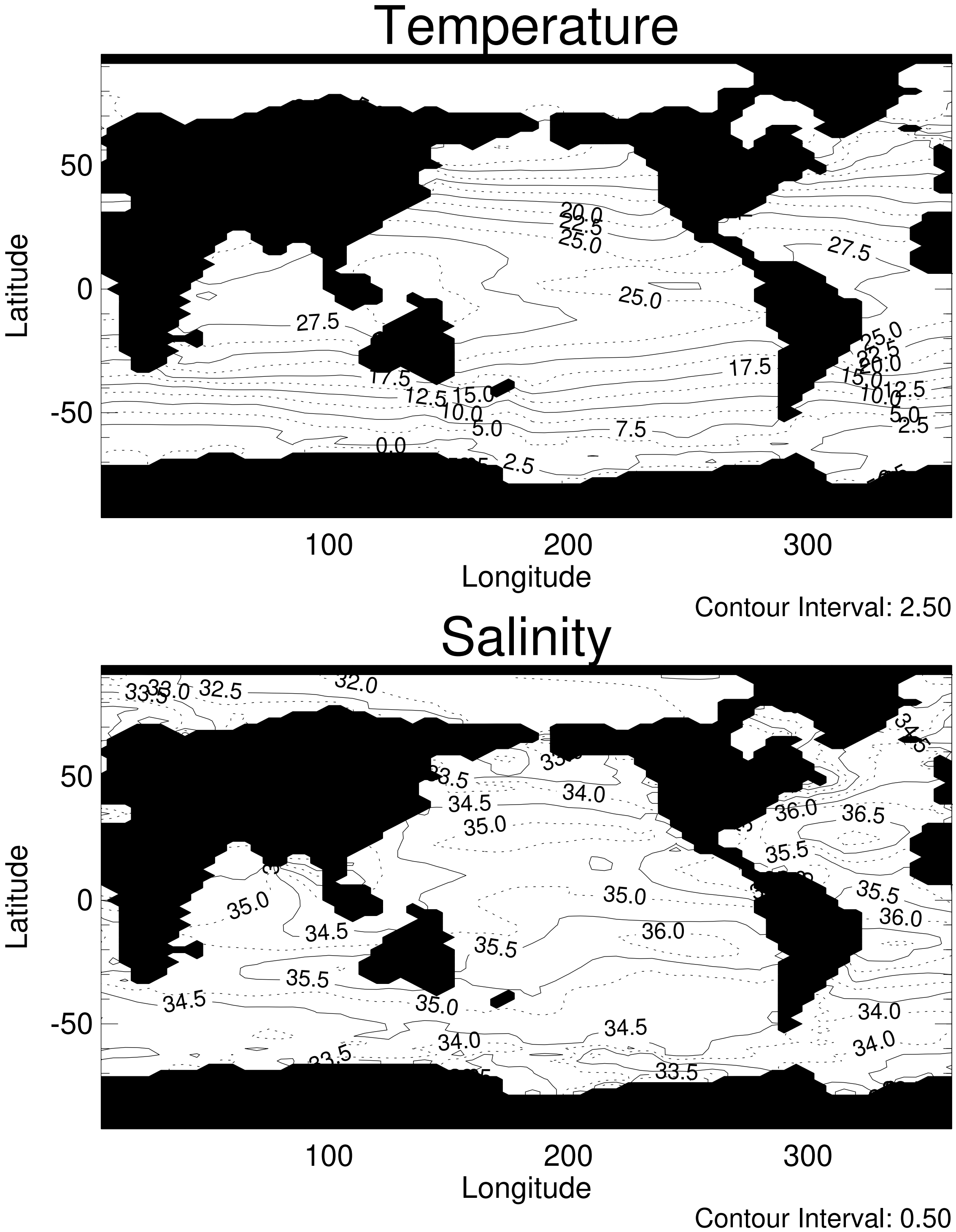
Temperature
Latitude
Longitude
50
0
-50
100
200
300
27.5
25.0
17.5
7.5
5.0
2.5
0.0
Contour Interval: 2.50
Salinity
Latitude
Longitude
50
0
-50
100
200
300
32.5
32.0
34.0
34.5
35.0
35.5
36.0
36.5
33.5
Contour Interval: 0.50

Figure 5:

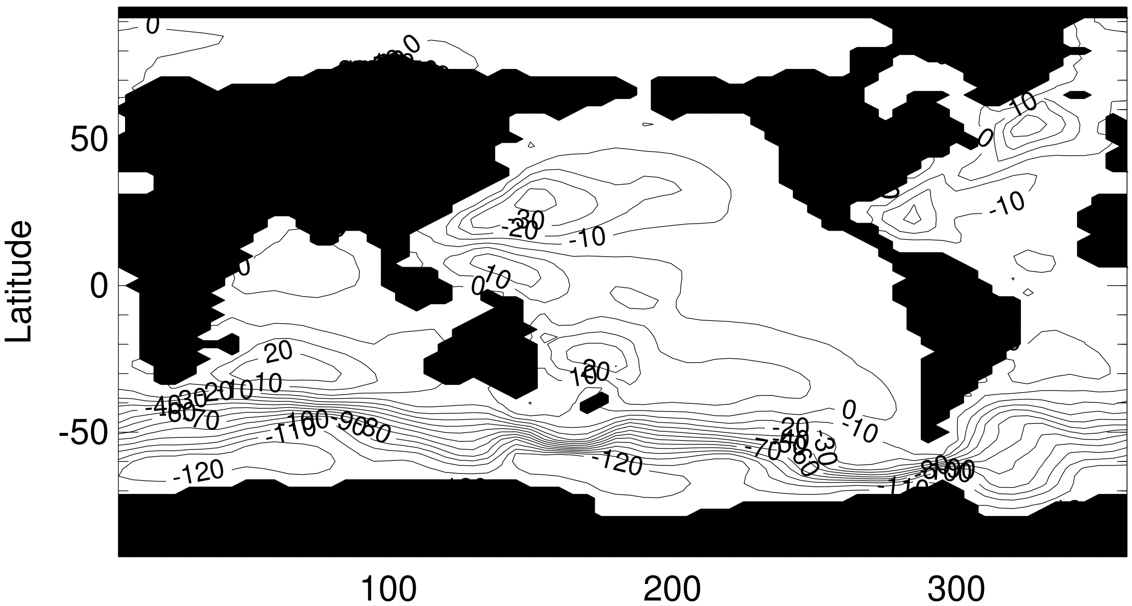

Figure 6:

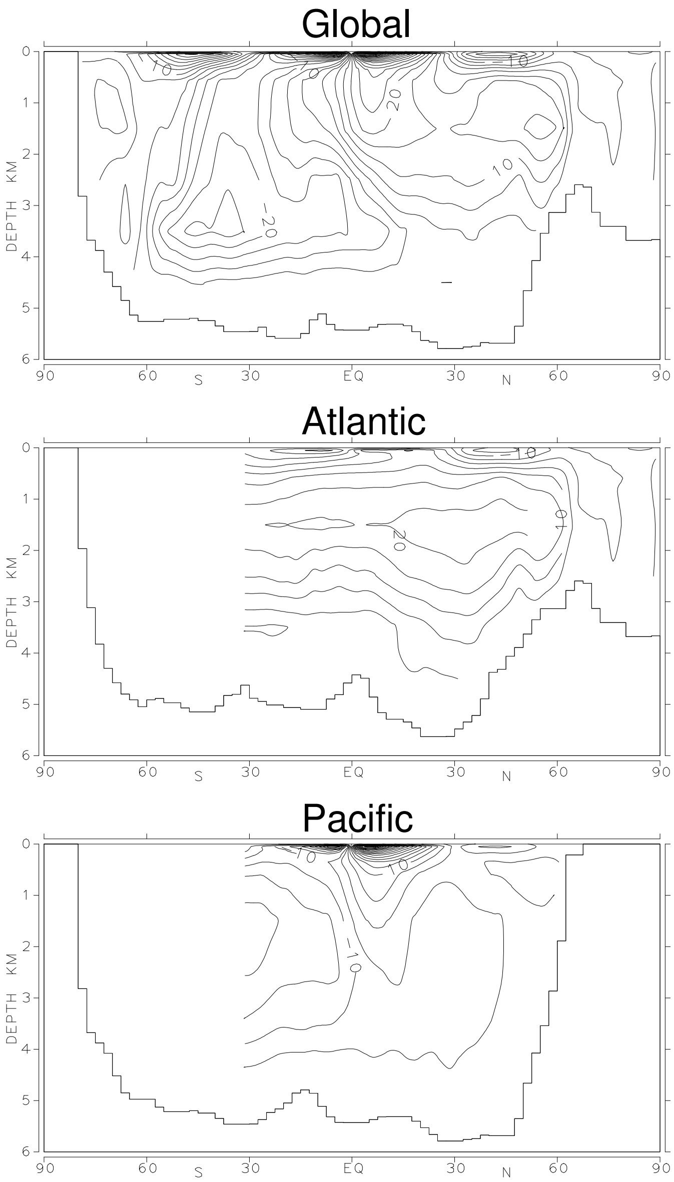

Figure 7:

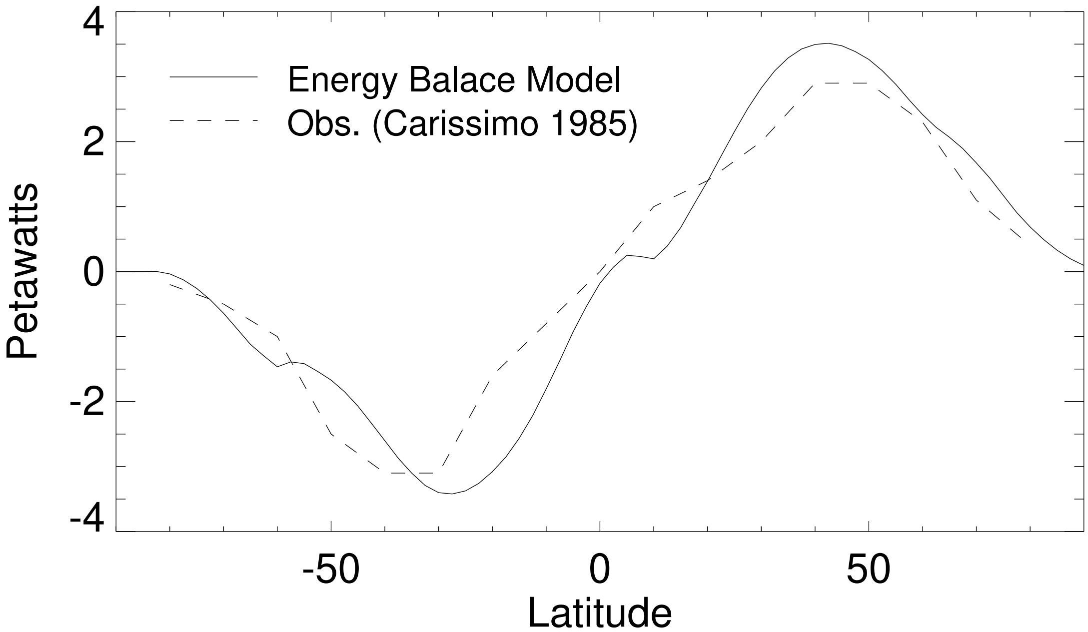
Energy Balace Model
Obs. (Carissimo 1985)
Petawatts
Latitude
4
2
0
-2
-4
-50
0
50

Figure 8:

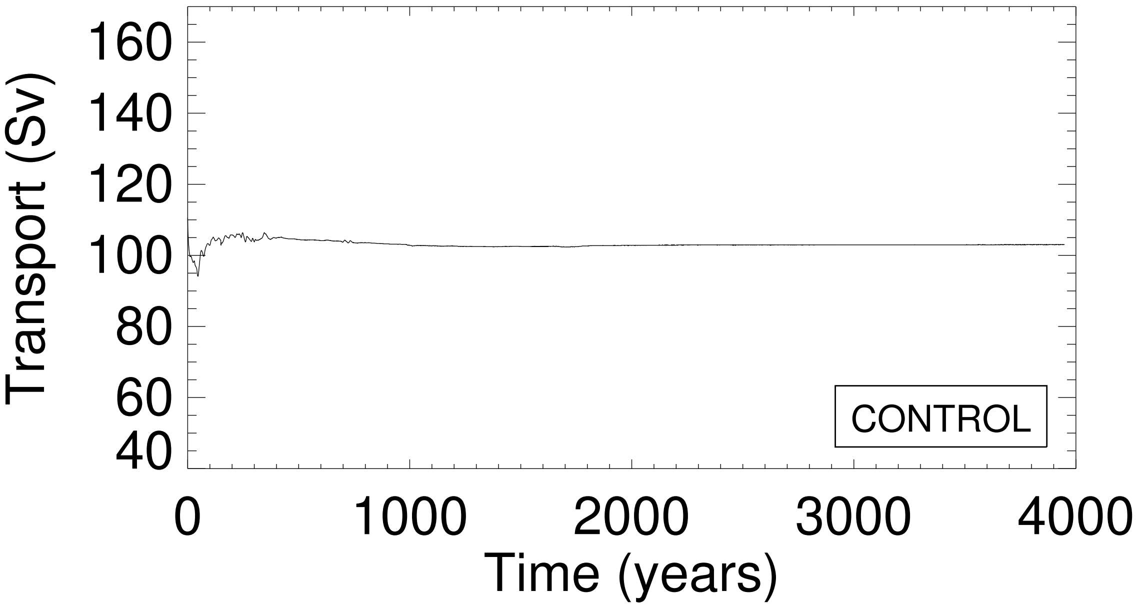
Transport (Sv)
160
140
120
100
80
60
40
0
1000
2000
3000
4000
Time (years)
CONTROL

Figure 9:

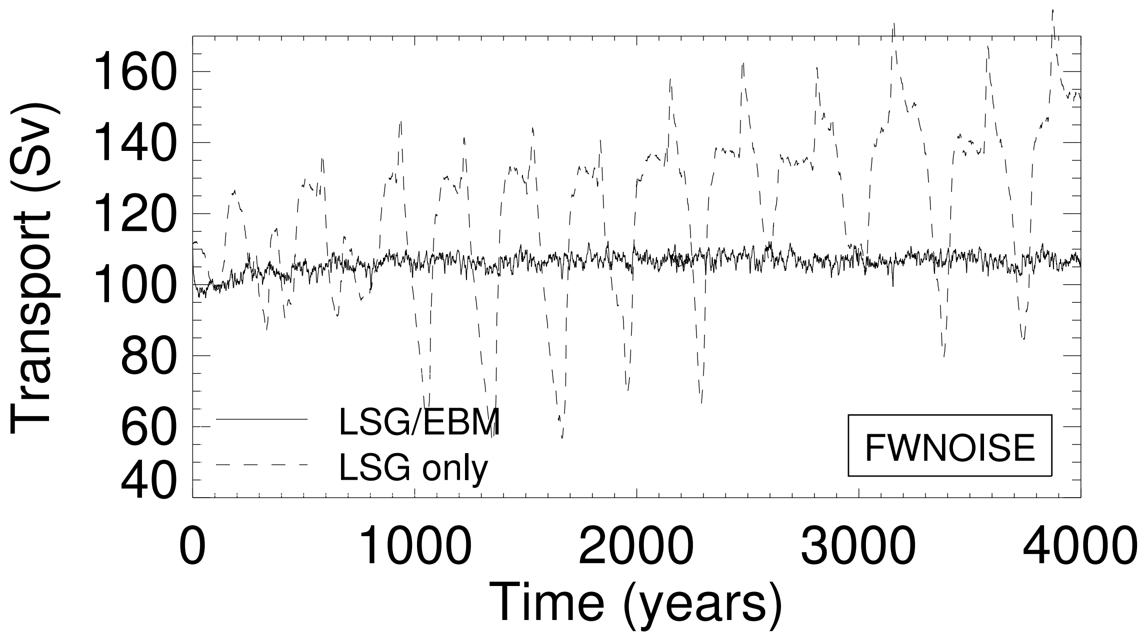
160
140
120
100
80
60
40
Transport (Sv)
0
1000
2000
3000
4000
Time (years)
LSG/EBM
LSG only
FWNOISE

Figure 10:

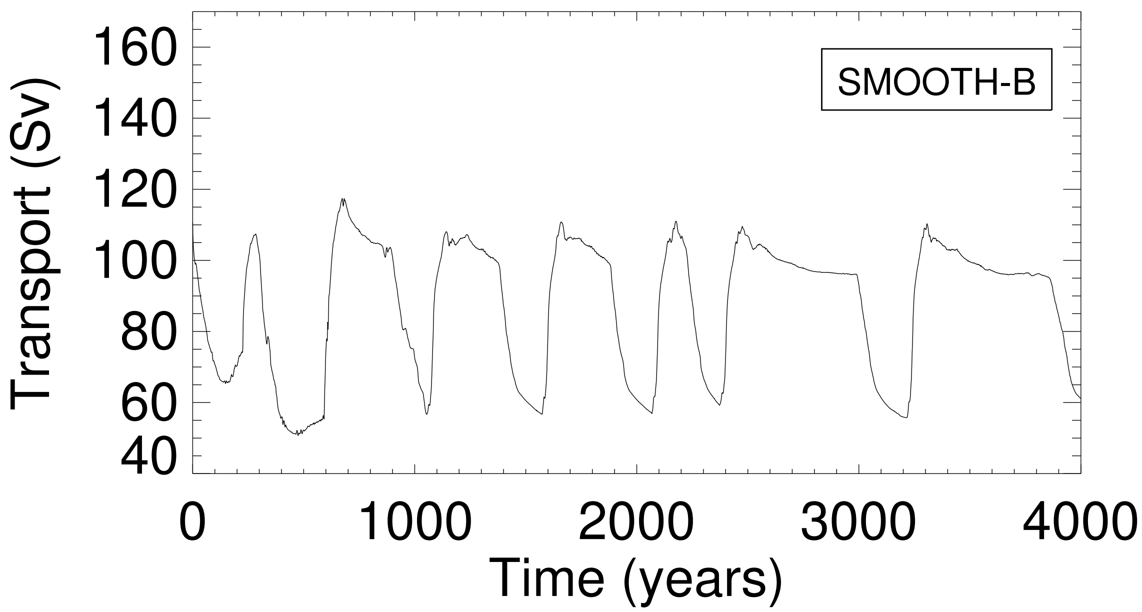
SMOOTH-B
Transport (Sv)
160
140
120
100
80
60
40
0
1000
2000
3000
4000
Time (years)

Figure 11:

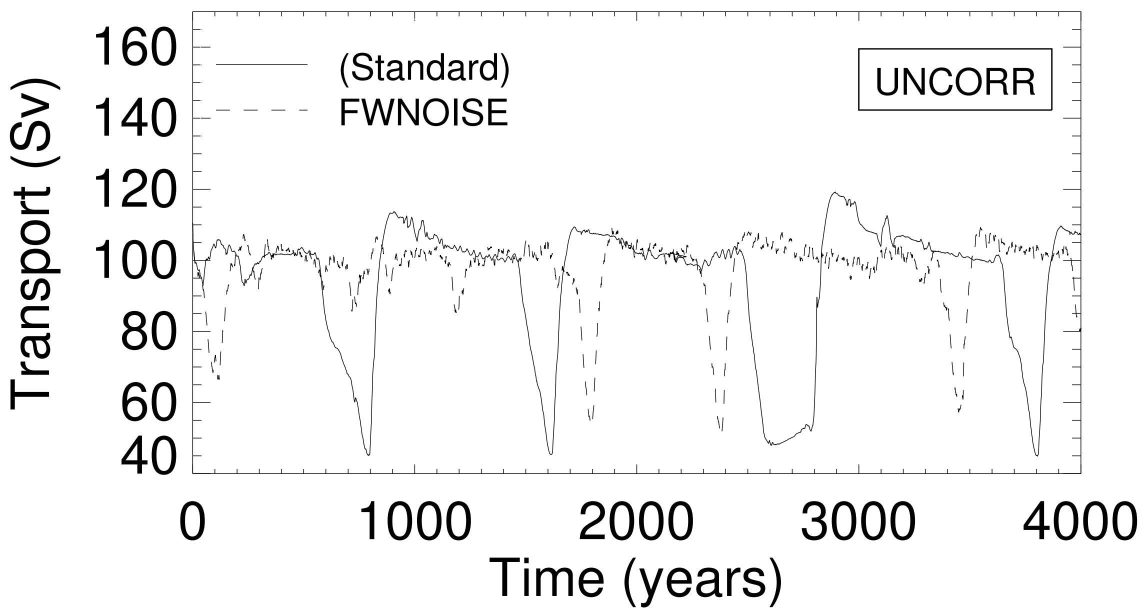
(Standard)
FWNOISE
UNCORR
Transport (Sv)
160
140
120
100
80
60
40
0
1000
2000
3000
4000
Time (years)

Figure 12:

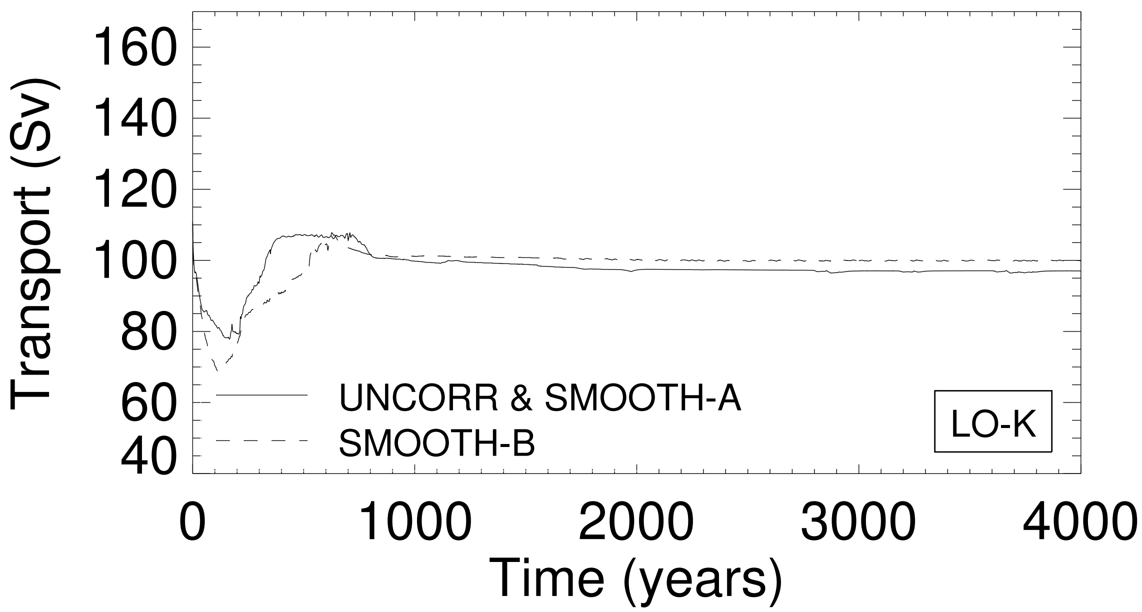

Transport (Sv)
160
140
120
100
80
60
40
0
1000
2000
3000
4000
Time (years)
UNCORR & SMOOTH-A
SMOOTH-B
LO-K

Figure 13:

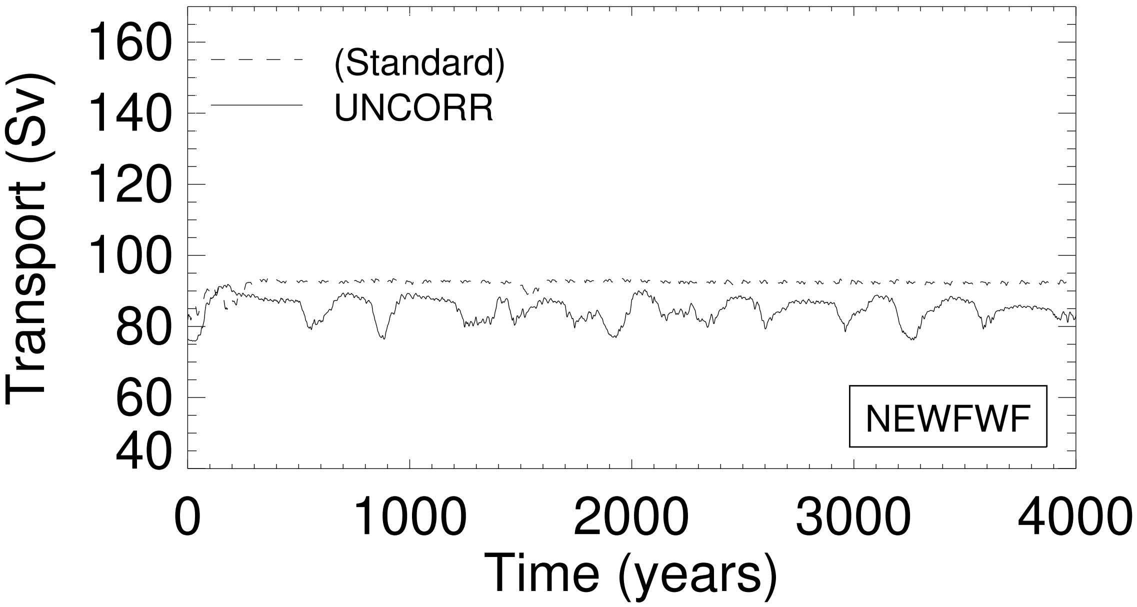

Transport (Sv)
160
140
120
100
80
60
40
(Standard)
UNCORR
NEWFWF
0
1000
2000
3000
4000
Time (years)

Figure 14:

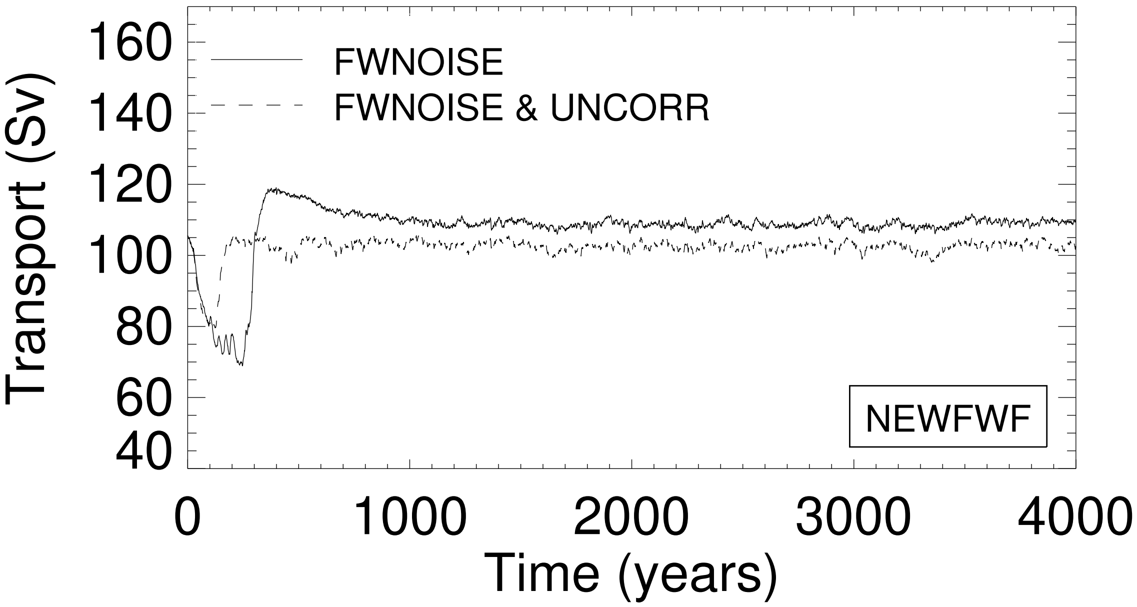
FWNOISE
FWNOISE & UNCORR
NEWFWF
Transport (Sv)
160
140
120
100
80
60
40
0
1000
2000
3000
4000
Time (years)

Figure 15:

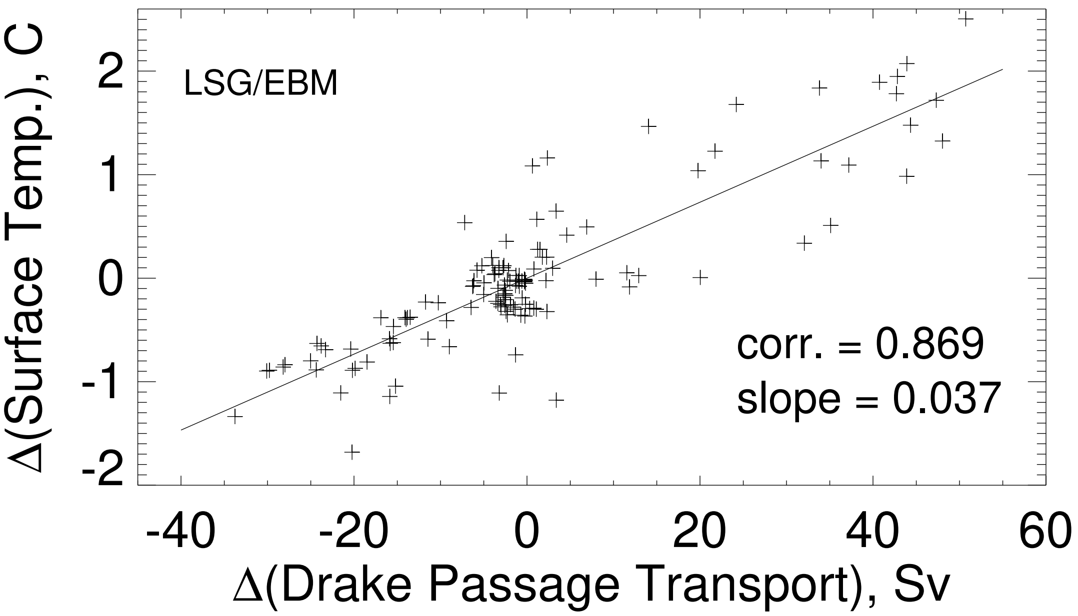
LSG/EBM
corr. = 0.869
slope = 0.037
Δ(Surface Temp.), C
Δ(Drake Passage Transport), Sv
2
1
0
-1
-2
-40
-20
0
20
40
60

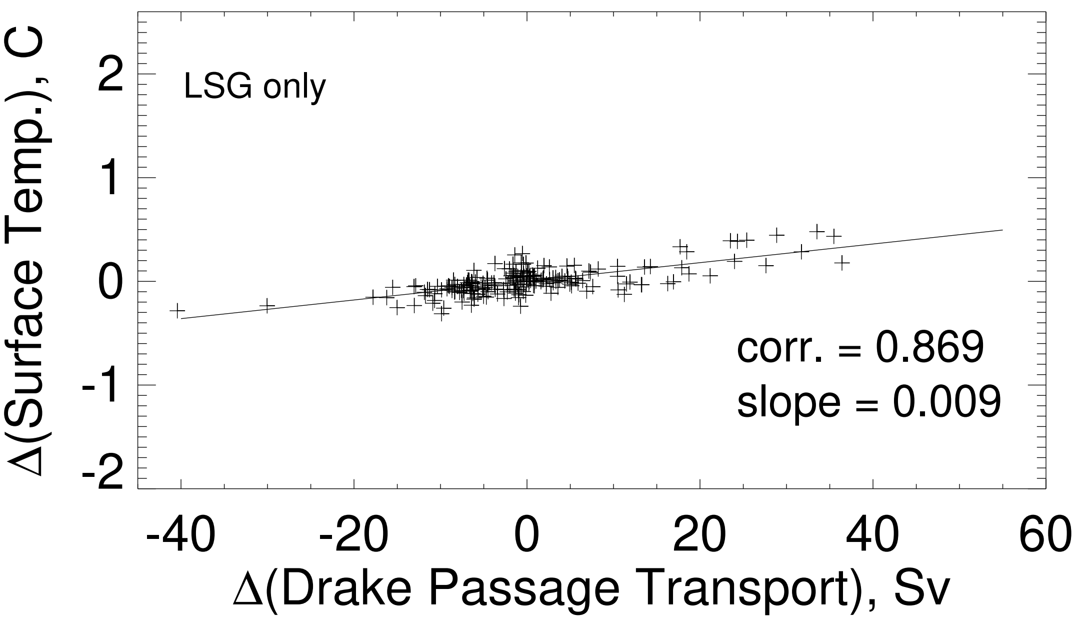
LSG only
corr. = 0.869
slope = 0.009
Δ(Surface Temp.), C
Δ(Drake Passage Transport), Sv
2
1
0
-1
-2
-40
-20
0
20
40
60

Figure 16:

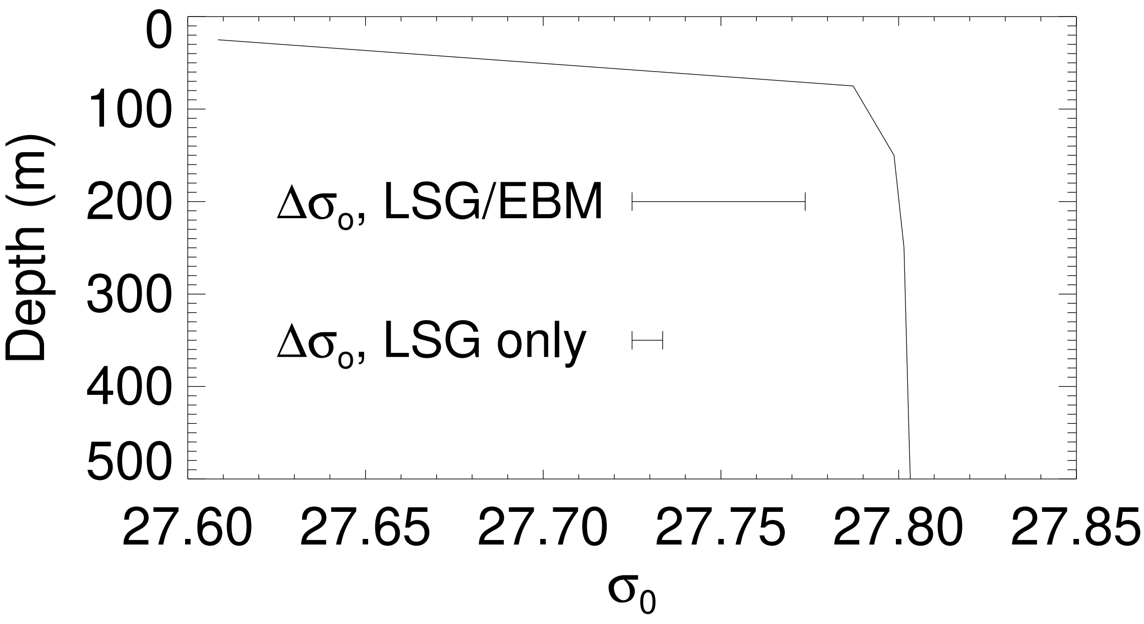

0
100
200
300
400
500
Depth (m)
Δσo, LSG/EBM
Δσo, LSG only
27.60
27.65
27.70
27.75
27.80
27.85
σ0

Figure 17:

Other citations:

Genthon (1994)